Resistivity and magnetoresistance properties of R_2NiSi_3 (R = Gd, Dy, Ho, Er, Tm) compounds

Santanu Pakhira[a,b,*], R. Ranganathan[a], Chandan Mazumdar[a]

[a] *Condensed Matter Physics Division, Saha Institute of Nuclear Physics, 1/AF, Bidhannagar, Kolkata 700064, India*

[b] *Ames Laboratory-USDOE and Department of Physics and Astronomy, Iowa State University, Ames, Iowa 50011, USA*

Abstract

The resistivity and magnetoresistance behaviour of the hexagonal intermetallic compounds R_2NiSi_3 (R = Gd, Dy, Ho, Er, and Tm) are reported here. All the studied polycrystalline compounds exhibit metallic behaviour along with additional magnetic anomalies at low temperatures. A well-defined resistivity minima is observed in Gd_2NiSi_3 and $Dy_2Ni_{0.87}Si_{2.95}$ at a temperature much higher than their respective magnetic transition temperatures. The anomaly has been ascribed to the charge carrier localization caused by magnetic precursor effect. Magnetic field induced crossover from positive to negative magnetoresistance (MR) behaviour associated with antiferromagnetic ground state is evidenced for Gd_2NiSi_3 and Er_2NiSi_3 in the low temperature region. Although $Tm_2Ni_{0.93}Si_{2.93}$ does not exhibit any long range magnetic order down to 2 K, a sudden drop in resistivity behaviour is observed below ∼10 K. Presence of short range magnetic correlation observed in a wide temperature range, much beyond their respective magnetic ordering temperatures, has been argued to be responsible for achieving finite negative MR for all the compounds. A subtle resemblance between the observed transport anomalies and the magnetic properties of these systems have been discussed.

Keywords: Intermetallic alloys and compounds, Rare-earths, Magnetic materials, Resistivity, Magnetoresistance

1. Introduction

Rare-earth (R) based ternary intermetallic compounds, R_2TX_3 (T = transition metals, and X = Si, Ge), have attracted significant attention both from fundamental and application point of view due to manifestation of various interesting physical properties associated with complex structure-property relationship[1, 2, 3, 4, 5, 6, 7, 8, 9, 10, 11, 12]. Most of these compounds form in layered hexagonal AlB_2-type crystal structure with space group $P6/mmm$. In this structure, R ions are on the vertices of edge-sharing triangles forming a

*spakhira@ameslab.gov

hexagonal layer and in between two such layers, the T and X elements are randomly distributed in an intermediate plane[1]. The exchange interaction among the R ions is of Ruderman–Kittel–Kasuya–Yosida (RKKY) type and strongly depends on the nature of the conduction electron cloud around the R ions. The variation of local electronic environment among the R ions caused by random statistical distribution of T and X ions are found to be responsible for the emergence of various complex magnetic behaviour in many reported R_2TX_3 type of compounds with different transition elements[2, 3, 4, 5, 6, 7, 9, 10, 11, 13, 14, 15, 16, 17].

The nature of complex magnetic interactions has also been reflected in the transport properties in few of these compounds. For example, Gd_2PdSi_3 exhibits a resistivity minimum above the Néel temperature with a large negative magnetoresistance[18, 19]. A negligible substitution of of non-magnetic element, La, at the Ce site in the Kondo-lattice compound Ce_2CoSi_3 introduces non-Fermi liquid behaviour in the system[20]. Observation of large negative magnetoresistance is reported in Eu_2CuSi_3 above it's ferromagnetic (FM) ordering temperature[21]. $Sm_2Ni_{0.87}Si_{2.87}$ shows resistivity upturn at low-temperature associated with the quantum interference effect caused by the elastic electron-electron interaction[22, 23]. Though the magnetic properties of R_2TX_3 type of compounds have been extensively reported, relatively less attention were paid towards the investigation of their transport properties. Although one would certainly expect a wide range of intriguing transport phenomena in these systems, on the verge of complex magnetic interactions.

One such interesting example is the recent discovery of field-induced skyrmionic phase in Gd_2PdSi_3, where the magnetic frustration is considered to be directly responsible for producing topological spin textures[12]. This work have generated pivotal interest in deep understanding of the magnetotransport properties of magnetically frustrated similar other systems. Research on magnetic skyrmions are presently considered to be of significant interest due to their potential applications in spintronics and also as information storage devices. One major common feature found in Gd_2PdSi_3 and many other members of intermetallic R_2TX_3 family is the magnetically frustrated ground state and magnetic field-induced associated metamagnetic transitions. These characteristics have been described as one of the key features for the development of field-induced skyrmionic spin texture in Gd_2PdSi_3[12]. Consequently, it creates an insatiable scientific urge to carry out the investigation on magnetotransport properties of different other isostructural members.

In this work, we report the basic resistivity and magnetoresistance (MR) behaviour of polycrystalline R_2NiSi_3 (R = Gd, Dy, Ho, Er, Tm) compounds which belong to the same R_2TX_3 family. It is reported that, among different members of R_2NiSi_3 compounds, Gd and Er-based analogue form in single phase with full stoichiometry[9], while vacancies in Ni and Si sites lead to single phase formation in case of other polycystalline compounds with R = Pr-Sm, Tb-Ho, and Tm[10, 11, 22, 24, 25, 26, 27]. All these compounds are reported to show different types of magnetic ground state depending upon the local electronic environment around the magnetic R ions. Crystal defects also play a crucial role in controlling the ground state properties of these systems. Here we report, the resistivity and MR properties of a few such members with R = Gd, Dy, Ho, Er, & Tm and have discussed a subtle correlation between the observed transport properties with their magnetic behaviour.

Table 1: Room-temperature crystallographic data for R_2NiSi_3 (R = Gd, Dy, Ho, Er, Tm) compounds obtained from XRD and SEM-EDX analysis.

Compound	Unit cell parameters		Estimated composition	
	a (Å)	c (Å)	XRD	SEM-EDX
Gd_2NiSi_3	3.983(2)	4.098(3)	$Gd_2Ni_{1.02(1)}Si_{2.99(1)}$	$Gd_2Ni_{0.99(2)}Si_{3.00(4)}$
$Dy_2Ni_{0.87}Si_{2.95}$	3.959(1)	4.026(1)	$Dy_2Ni_{0.90(1)}Si_{2.95(1)}$	$Dy_2Ni_{0.94(2)}Si_{3.02(3)}$
$Ho_2Ni_{0.95}Si_{2.95}$	3.953(2)	4.000(1)	$Ho_2Ni_{0.95(1)}Si_{2.95(1)}$	$Ho_2Ni_{0.93(2)}Si_{2.98(5)}$
Er_2NiSi_3	3.996(2)	3.972(1)	$Er_2Ni_{1.00(1)}Si_{3.00(1)}$	$Er_2Ni_{1.00(1)}Si_{3.00(3)}$
$Tm_2Ni_{0.93}Si_{2.93}$	3.936(1)	3.953(1)	$Tm_2Ni_{0.97(1)}Si_{2.98(2)}$	$Tm_2Ni_{0.95(2)}Si_{3.00(2)}$

2. Experimental details

The polycrystalline compounds were prepared using standard arc-melting technique under argon atmosphere in an arc furnace. For homogenization, the samples were melted 5-6 times by flipping after each melt. The structural characterization were done by x-ray diffraction (XRD) studies. Scanning electron microscopy (SEM) and the energy dispersive x-ray spectroscopy (EDX) measurements were done in the instrument EVO 18 (M/s Carl Zeiss, Germany) equipped with a EDX system (M/s EDAX Inc., USA). The magnetic and transport measurements were carried out in a superconducting quantum interference device (SQUID) (M/s Quantum Design Inc., USA) and PPMS EverCool-II (M/s Quantum Design Inc., USA) in the temperature range 2–300 K and magnetic fields up to 9 T (1 T $\equiv 10^4$ Oe). The electrical resistivity measurements were performed using standard four-probe technique. The samples were prepared in a shape of parallelepiped by polishing the surfaces and care was taken to make the surface uniform with minimum surface roughness. Silver epoxy was used for making the electrical contacts between the leads with the sample surface. The possibility of having small errors associated with the measured absolute value of resistance, that may come due to the micro cracks developed in these polycrystalline samples during polishing, can not be ruled out completely.

3. Results and Discussions

The structural characterizations of all the compounds have been carried out by analyzing the room-temperature XRD data using FullProf software package[28]. Phase homogeneity and the average compositions have also been verified though SEM-EDX analysis. All the structural parameters estimated from these measurements are listed in Table 1. All the studied compounds form in single phase having hexagonal AlB_2-type crystal structure with space group $P6/mmm$. No trace of secondary phase could be detected within the resolution limit of the instruments in any of these experiments. The detailed structural analysis along with corresponding data have already been reported in Refs.[[9, 10, 26, 27]].

The temperature dependence of zero-field resistivity data, $\rho(T)$, measured in the temperature range 2–300 K is shown in Fig. 1(a). It is reported that polycystalline Gd_2NiSi_3 exhibits AFM transition below $T_N = T_f = 16.4$ K coupled with spin-glass transition[9], as

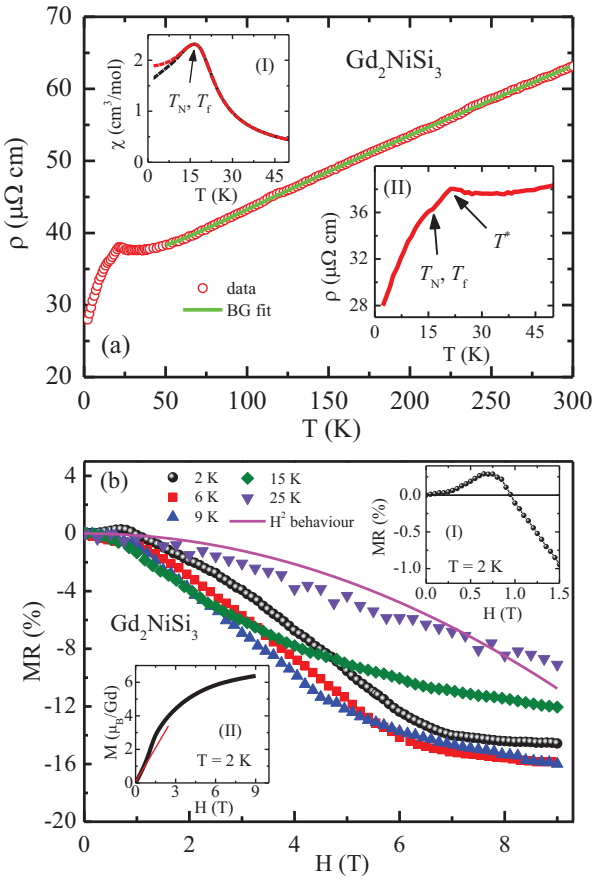

Figure 1: (a) Zero-field $\rho(T)$ behaviour of Gd_2NiSi_3 along with the fit using Eq. 1 in the paramagnetic region. Inset (I): low temperature dc magnetic susceptibility in ZFC (black line) and FC mode (red line) for $H = 0.1$ T. Inset (II): Expanded low T region of $\rho(T)$. (b) Magnetoresistance, MR, as a function of applied field measured at different temperatures. Inset (I): Expanded low H region of MR at $T = 2$ K. Inset (II): $M(H)$ behaviour of the compound at $T = 2$ K.

shown in inset (I) of Fig. 1(a). The $\rho(T)$ gradually decreases with temperature down to 35 K yielding a metallic behaviour, below which it shows an upward tendency. Upon further cooling resistivity decreases below $T^* \sim 20$ K, which is higher than the Néel temperature of the compound (Inset (II): Fig. 1(a)). A small kink could also be observed at T_N indicating the onset of magnetic ordering in the system and below which $\rho(T)$ decreases due to the loss of spin-disorder scattering. The estimated residual resistivity ratio RRR $\equiv \rho(300\text{ K})/\rho(2\text{ K})$ ≈ 2.25 for this compound and is similar to that observed for different other isostructural members[18, 19, 30].

The observation of resistivity minima above the Néel temperature are a typical signature of Kondo-lattice system and often observed in many related Ce-based compounds[29]. The Kondo effect, however can be ruled out in the present system as the $4f$ orbital of Gd ions are localized deep below the Fermi energy. In many AFM compounds, resistivity upturn below the ordering temperature are also observed due to the formation of superzone energy

gap, whereas in case of Gd_2NiSi_3 such upturn is observed at a higher temperature than T_N. Similar behaviour had also been observed for isostructural Gd_2PdSi_3 and it was argued that magnetic precursor effect associated with electron localization in this magnetic system might be responsible for such observation[18], which also may be the situation in Gd_2NiSi_3. It is quite possible that the increase in resistivity due to this precursor effect compete with the loss of spin-disorder scattering as one approaches T_N from the high T limit, and finally ρ decreases below T^* where the later contribution dominates. It may be mentioned here that a considerable amount of magnetic entropy change associated with magnetic precursor effect is also observed for this compound in a wide temperature range, much beyond the magnetic ordering temperature[9].

The $\rho(T)$ behaviour of a metallic system in the paramagnetic region is described by Bloch-Grüneisan (BG) model, given by

$$\rho_{\rm BG}(T)=\rho_0+F\left(\frac{T}{\Theta_R}\right)^5 \int_0^{\theta_R/T} \frac{x^5 dx}{(1-e^{-x})(e^x-1)}, \quad (1)$$

where, F is a numerical constant which describes the T-independent interaction strength of the conduction electrons with the thermally excited phonons, and contains the ionic mass, Fermi velocity, and other parameters, $x = \frac{h\omega}{2\pi k_B T}$, Θ_R is the Debye temperature estimated from resistivity studies. The $\rho_{\rm BG}(T)$ can be represented as an accurate analytic Padé approximant function of T/Θ_R [31]. It is evident from Fig. 1(a) that the $\rho(T)$ behaviour in Gd_2NiSi_3 could be well described by BG model in the T range 50–300 K and the estimated parameters are listed in Table. 2.

The effect of external magnetic field (H) on the electronic transport properties of Gd_2NiSi_3 have been studied by measuring the resistance as a function of H at different temperatures (both above and below the magnetic transition temperature). The estimated magnetoresistance, MR$(H,T)\equiv [\rho(H,T)-\rho(0,T)]/\rho(0,T)$ is plotted in Fig. 1(b). The MR behaviour at $T = 2$ K, is found to be positive for $H < 1$ T (Inset (I): Fig. 1(b)) and above that it is negative with a saturation tendency for $H > 7$ T. A positive MR value generally signifies the presence of strong AFM interaction in a system. In case of Gd_2NiSi_3 the magnetic ground state also consists of antiferromagnetically coupled spins and with increase in magnetic field strength, field-induced ferromagnetism appears. A similar field-dependent magnetoresistance behaviour had earlier been reported in some members of $R_2Ni_3Si_5$ compounds (R = Pr, Dy, Ho), and also argued to have originated from the metamagnetic behaviour associated with short-range ferromagnetic interactions[32, 33]. The $M(H)$ behaviour of Gd_2NiSi_3 at 2 K (Inset (II): Fig. 1(b)) is linear up to 1 T magnetic field and after that the magnetization increases rapidly signifying the polarization of the magnetic spins in the field direction with a saturation tendency at higher field region. Thus, the observed magnetoresistance behaviour are also in the same line to the reported isothermal magnetization behaviour in Gd_2NiSi_3[9].

The maximum value of negative MR observed at $T = 2$ K is $\sim$ – 14.5% for $H = 9$ T. The MR values for all other temperatures are found to be negative in the measured field range, though the selected temperatures, 6, 9, and 15 K remain smaller than the T_N of the compound. The maximum value of estimated MR is $\sim$ – 16% at $T = 9$ K. Interestingly, the observation of significant MR value at $T = 25$ K ($> T_N, T^*$) indicates that the zero-field resistivity minima caused by magnetic precursor effect strongly depends on the applied

magnetic field and reduces with increasing field strength. Furthermore, MR behaviour at 25 K does not follow H^2 dependence which is a manifestation of external H effect on the paramagnetic spins and thus expected in a true paramagnetic region[34, 35]. Rather large value of MR, although positive, in the paramagnetic region was also reported earlier in some of the $R_2Ni_3Si_5$ type of compounds (R = Tb, Sm, Nd), and interpreted to have structural origin[36]. It should be mentioned here that, the magnetic measurements also reveal the presence of short range magnetic correlation in Gd_2NiSi_3 at least up to 60 K[9]. Thus, both the electronic transport and magnetization measurements are found to be complementary to each other.

Table 2: The parameters obtained from Bloch Grüneisen and Parallel resistor fit, by using Eq.1 (for R = Gd) and Eq. 2 (for R = Dy, Ho, Er, and Tm) respectively, to $\rho(T)$ data of R_2NiSi_3 compounds in the paramagnetic region

Compound	RRR	ρ_0 ($\mu\Omega$ cm)	$\rho_{\max}$ ($\mu\Omega$ cm)	F ($\mu\Omega$ cm)	Θ_R (K)
Gd_2NiSi_3	2.25	37.08(6)		23.8(3)	275(4)
$Dy_2Ni_{0.87}Si_{2.95}$	1.39	51.4(2)	162(2)	20.1(4)	210(2)
$Ho_2Ni_{0.95}Si_{2.95}$	1.35	51(1)	253(9)	33(1)	408(4)
Er_2NiSi_3	1.46	50.4(2)	306(6)	21.8(4)	246(3)
$Tm_2Ni_{0.93}Si_{2.93}$	2.02	24.2(1)	130(1)	12.9(2)	188(2)

The zero-field $\rho(T)$ behaviour in the T range 2–300 K of $Dy_2Ni_{0.87}Si_{2.95}$ is shown in Fig. 2(a). Magnetic measurements reported for this compound reveal the presence of cluster glass state formation below $T_f = 5.6$ K[26] (Inset (I): Fig. 2(a)). However, the presence of distinct peak in the zero-field heat capacity data at the same temperature and negative value of paramagnetic Weiss temperature ($\theta_p = -3.9$ K) also indicates the coexistence of AFM phase along with glassy phase. Such phase coexistence have already been revealed through neutron diffraction measurements for some of the members of R_2NiSi_3 family[9, 25]. The $\rho(T)$ behaviour of $Dy_2Ni_{0.87}Si_{2.95}$ yields that the compound is metallic in nature with RRR $\equiv \rho(300\text{ K})/\rho(2\text{ K}) \approx 1.39$, which is lower than that estimated for the Gd-based analogue. As the temperature is lowered below a characteristic temperature $T_m \sim 11.2$ K, which is slightly higher than the ordering temperature of the compound, the resistivity starts to increase (Inset (II): Fig. 2(a)). No additional anomaly could be observed in the $\rho(T)$ data at T_f. The reported magnetic and zero-field heat capacity studies of $Dy_2Ni_{0.87}Si_{2.95}$ indicate the presence of substantial short range magnetic correlation up to much higher temperature than the magnetic ordering temperature, that in turn results in large entropy change in the system above T_f[26]. Thus the resistivity upturn below T_m is also likely to be associated with the magnetic Brillouin-zone boundary gap opening due to the growth of AFM interaction in the system. In such scenario, magnetic sublattice distorts the Fermi surface resulting a gap

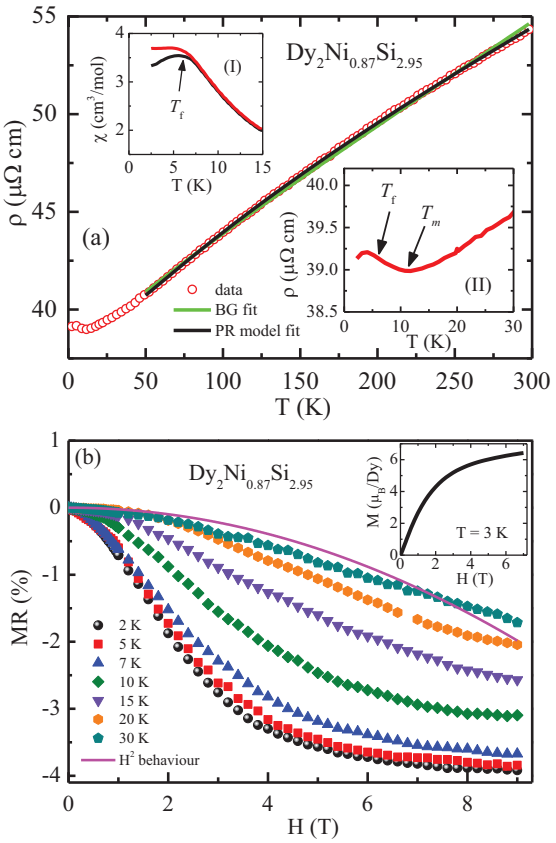

Figure 2: (a) Zero-field $\rho(T)$ behaviour of $Dy_2Ni_{0.87}Si_{2.95}$ along with the fit using Eq. 1 (green solid line) and Eq. 2 (black solid line) in the paramagnetic region. Though two different fits are hard to distinguish on the scale of the figures, careful observation reveal considerable discrepancies. Inset (I): Low temperature dc magnetic susceptibility in ZFC (black line) and FC mode (red line) for $H = 0.05$ T. Inset (II): Expanded low T region of $\rho(T)$. (b) Magnetoresistance, MR, as a function of applied field measured at different temperatures. Inset: $M(H)$ behaviour of the compound at $T = 3$ K.

opening in the conduction band, which in turn is responsible for the increase in $\rho(T)$ with decreasing temperature, similar to that found in a few other isostructural analogues[4, 37]. The resistivity decreases with temperature below 4 K due to the reduction in spin-disorder scattering.

The paramagnetic $\rho(T)$ behaviour could not be described by BG model with good accuracy due to the negative curvature for $T \geq 75$ K, as shown in Fig. 2(a). Such type of negative curvature in the $\rho(T)$ data of many metallic compounds arise due to the presence of crystalline electric field (CEF) or interband scattering of the conduction electrons[38]. A phenomenological model that can best describe the negative curvature in the paramagnetic $\rho(T)$ data is parallel-resistor (PR) model[39] given by,

$$\frac{1}{\rho(T)} = \frac{1}{\rho_{BG}(T)} + \frac{1}{\rho_{max}(T)} \tag{2}$$

where ρ_{max} is temperature independent saturation resistivity, also known as the Ioffe-Regel

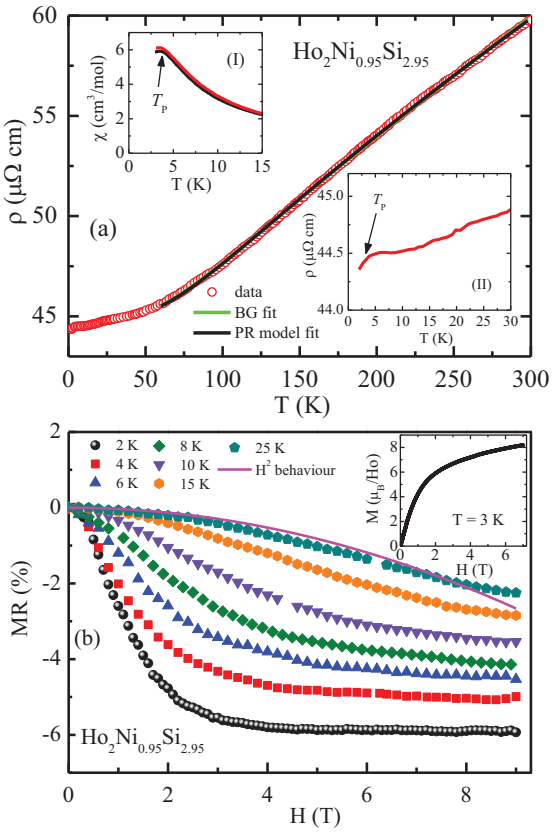

Figure 3: (a) Zero-field $\rho(T)$ behaviour of $Ho_2Ni_{0.95}Si_{2.95}$ along with the fit using Eq. 1 (green solid line) and Eq. 2 (black solid line) in the paramagnetic region. Though two different fits are hard to distinguish on the scale of the figures, careful observation reveal considerable discrepancies. Inset (I): Low temperature dc magnetic susceptibility in ZFC (black line) and FC mode (red line) for $H = 0.05$ T. Inset (II): Expanded low T region of $\rho(T)$. (b) Magnetoresistance, MR, as a function of applied field measured at different temperatures. Inset: $M(H)$ behaviour of the compound at $T = 3$ K.

resistivity [40] and ρ_{BG} is the Bloch Grüneisen form of resistivity. As seen from the figure, the $\rho(T)$ behaviour in the temperature region 50–300 K could be well fitted using the PR model. The different estimated parameters are summarized in Table. 2.

The MR behaviour measured at different temperatures of $Dy_2Ni_{0.87}Si_{2.95}$ are shown in Fig. 2(b). The MR values found to be negative down to the lowest measured temperature and the maximum magnitude attains a value of $\sim -3.95\%$ at $T = 2$ K for 9 T magnetic field. The magnetic measurements for the compound reveals that the ground state spin configuration is fragile in nature and very much susceptible to the applied magnetic field (Inset: Fig. 2(b)). Such signature could also be traced from the low temperature MR behaviour that shows saturation tendency in the higher field region. The MR behaviour measured at 30 K also does not exhibit H^2 dependence signifying that the true paramagnetic region is still in the higher temperature side, similar to that observed in magnetic behaviour of the system[26].

Figure 3(a) depicts the zero-field $\rho(T)$ data of $Ho_2Ni_{0.95}Si_{2.95}$. The resistivity decreases with temperature as expected for a metallic system and the RRR value $\equiv \rho(300\text{ K})/\rho(2\text{ K})$

≈ 1.35. No significant anomaly could be found in the $\rho(T)$ behaviour except the observation of a very weak hump around $T_P \sim 3.6$ K (Inset II: Figure 3(a)). It is reported that though the low field magnetic susceptibility of $Ho_2Ni_{0.95}Si_{2.95}$ exhibits a weak peak around T_P (Inset I: Figure 3(a)), the heat capacity, ac susceptibility, and neutron diffraction studies rule out the possibility of any long-range magnetic ordering or spin freezing behaviour in the system[10]. The $\rho(T)$ behaviour for $T \geq 110$ K exhibits a weak negative curvature and thus the paramagnetic resistivity behaviour could be best described by PR model rather than BG model. The rate of decrease in resistivity value with respect to temperature is found to be lower for $2 \leq T \leq 30$ K, as compared to other members of this series. It may be mentioned here that the heat capacity behaviour also shows a broad anomaly in the temperature range 3–25 K with a sharp drop below 3 K[10]. The observed broad anomaly gets suppressed by the application of magnetic field.

Figure 3(b) shows the MR behaviour of $Ho_2Ni_{0.95}Si_{2.95}$ measured at some selected temperatures. The MR values are found to be negative with the most prominent one estimated at the lowest measured temperature (2 K) as $\sim -5.9\%$ for 9 T applied magnetic field. The MR values at 2 K tends to saturate for $H \gtrsim 2$ T and this is quite similar to the $M(H)$ behaviour where moments try to get oriented in the field direction yielding saturation tendency around the same field region. The absolute MR value decreases with increase in temperature. Though the compound does not show any long range magnetic ordering or spin freezing down to 2 K, the MR behaviour at a temperature as high as 25 K is also not that expected for a true paramagnetic system. This may be due to presence of short range magnetic correlation in the system extended up to quite higher temperature range. In the absence of any true long range magnetic ordering, $Ho_2Ni_{0.95}Si_{2.95}$ is also reported to exhibit large magnetocaloric effect caused by short range magnetic correlation[10].

Er_2NiSi_3 undergoes AFM ordering below $T_N = 5.4$ K and reenters to cluster glass state below $T_f = 3$ K[9] (Inset (I): Fig. 4(a)). Fig. 4(a) shows the zero-field $\rho(T)$ data of the compound in the temperature range 2–300 K. The ρ value decreases with decreasing temperature down to 2 K, signifying a typical metallic behaviour. No additional anomaly could be detected around T_N or T_f in the $\rho(T)$ behaviour (Inset (II): Fig. 4(a)). Though the compound orders in incommensurate AFM structure, the neutron diffraction results revealed that the magnetic coherence length is only limited to few unit cells[9]. The estimated positive value of Weiss temperature ($\theta_p = 0.8$ K) is also in the same line to the incommensurate structure that is associated with considerable amount of FM interaction in the system. Negligible value of θ_p stands for strongly competing nature of AFM and FM components in this system. This may be the reason for the absence of any anomaly (superzone gap) associated with AFM ordering around T_N in the $\rho(T)$ behaviour. The RRR $\equiv \rho(300\text{ K})/\rho(2\text{ K})$ value is found to be ~ 1.46, quite similar to that obtained for Dy, and Ho-based analogue. Similar to $Ho_2Ni_{0.95}Si_{2.95}$, very weak negative curvature in $\rho(T)$ data could be evidenced $T \geq 80$ K. The $\rho(T)$ behaviour has been fitted with both BG and PR model and the later one best describe the experimental data in the paramagnetic region, 50–300 K, as shown in Fig. 4(a).

The MR behaviour measured at different temperatures for Er_2NiSi_3 are plotted in Fig. 4(b). Very low positive MR values are obtained for $T < T_N$ for applied magnetic field $H \lesssim 0.4$ T. Such behaviour is consistent with AFM type ground state of the compound as revealed by

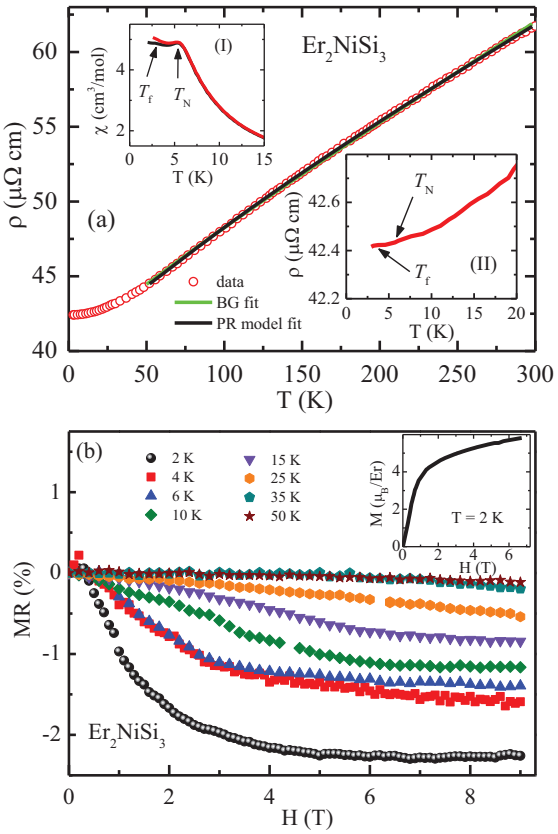

Figure 4: (a) Zero-field $\rho(T)$ behaviour of Er_2NiSi_3 along with the fit using Eq. 1 (green solid line) and Eq. 2 (black solid line) in the paramagnetic region. Though two different fits are hard to distinguish on the scale of the figures, careful observation reveal considerable discrepancies. Inset (I): Low temperature dc magnetic susceptibility in ZFC (black line) and FC mode (red line) for $H = 0.1$ T. Inset (II): Expanded low T region of $\rho(T)$. (b) Magnetoresistance, MR, as a function of applied field measured at different temperatures. Inset: $M(H)$ behaviour of the compound at $T = 2$ K.

magnetic and neutron diffraction data[9]. However, due to the presence of competing FM and AFM exchange interaction strength, $M(H)$ behaviour (Inset: Fig. 4(b)) deviates from linearity for $H > 0.5$ T indicating the field induced FM nature and thus yields negative MR at higher fields. MR values almost saturate at higher applied fields with a maximum obtained value of $\sim -2.25\%$ for $H = 9$ T at 2 K. The values of MR at higher temperatures become very small and thus we have not attempted to fit the data in search for H^2-dependence.

The $\rho(T)$ behaviour of $Tm_2Ni_{0.93}Si_{2.93}$ in the absence of any magnetic field is shown in Fig. 5(a). The $\rho(T)$ data confirms the metallic character of the system with RRR $\equiv \rho(300\text{ K})/\rho(2\text{ K})$ value ~ 2.02. Though the basic magnetic and heat capacity measurements reveal the absence of any magnetic ordering down to 2 K in the compound[27] (Inset (I): Fig. 5(a)), $\rho(T)$ manifests a sudden drop below $T < 10$ K. It may be mentioned here that the estimated negative value of paramagnetic Weiss temperature ($\theta_p = -3.7$ K) indicates the presence of dominant AFM interaction, although no magnetic ordering could be observed

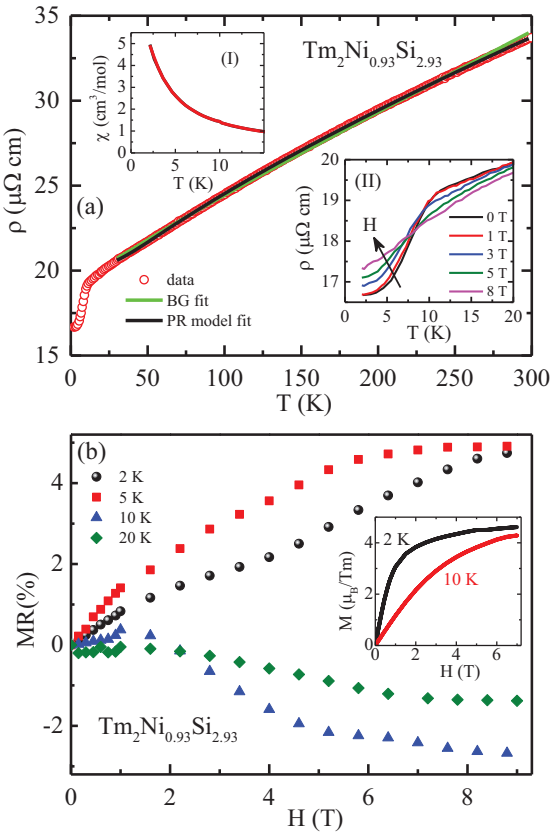

Figure 5: (a) Zero-field $\rho(T)$ behaviour of $Tm_2Ni_{0.93}Si_{2.93}$ along with the fit using Eq. 1 (green solid line) and Eq. 2 (black solid line) in the paramagnetic region. Though two different fits are hard to distinguish on the scale of the figures, careful observation reveal considerable discrepancies. Inset (I): Low temperature dc magnetic susceptibility in ZFC (black line) and FC mode (red line) for $H = 0.05$ T. Inset (II): Expanded low T region of $\rho(T)$ for different H. The arrow indicates increasing magnetic field direction. (b) Magnetoresistance, MR, as a function of applied field measured at different temperatures. Inset: $M(H)$ behaviour of the compound at $T = 2$ and 10 K.

down to 2 K.

The drop in $\rho(T)$ below 10 K also strongly depends on the external magnetic field as the anomaly gets suppressed with increasing field strength (Inset (II): Fig. 5(a)). Although we believe that one could gather more insight of complex magnetic interaction in $Tm_2Ni_{0.93}Si_{2.93}$ associated with this sudden drop in resistivity, the present set of experimental data is insufficient for further analysis. The $\rho(T)$ behaviour in the paramagnetic region ($T > 30$ K) could be well described by PR model compare to BG model due to the presence of finite negative curvature $T \geq 60$ K.

The measured MR behaviour of $Tm_2Ni_{0.93}Si_{2.93}$ are also quite different in nature than the other isostructural members, as depicted in Fig. 5(b). MR values at $T = 2$, and 5 K are found to be positive whereas the MR values for $T \geq 10$ K are negative. The observation of finite MR even at 10 K is in accordance with the nonlinear $M(H)$ behaviour (Inset: Fig. 5(b)) at that temperature indicating the influence of magnetic field on the short range magnetic

correlation in the system. Such correlation also results in large magnetocaloric effect in this system over a wide temperature region[27]. Thus, all these observations imply that there are conceptually open questions in understanding the microscopic magnetic behavior of $Tm_2Ni_{0.93}Si_{2.93}$ compound.

4. Summary

In summary, we report here the resistivity and magnetoresistance properties of the polycrystalline R_2NiSi_3 (R = Gd, Dy, Ho, Er, and Tm) compounds. All the studied compounds exhibit metallic behaviour and the observed transport properties are in good agreements to the reported magnetic behaviour of the systems. The $\rho(T)$ data of Gd_2NiSi_3 and $Dy_2Ni_{0.87}Si_{2.95}$ exhibit a well defined resistivity minima above their AFM transition temperatures that have been interpreted due to the magnetic precursor effect associated with charge carrier localization. No such anomaly could be observed around T_N of Er_2NiSi_3, that may be due to the presence of dominating FM interaction along with spatially restricted (low coherence length) AFM order. $\rho(T)$ behaviour does not show any additional anomaly at the spin freezing temperature of the compounds. In the absence of any magnetic ordering, resistivity behaviour of $Tm_2Ni_{0.93}Si_{2.93}$ suddenly drops below 10 K that get suppressed at the application of high magnetic field. Low temperature MR behaviour of Gd_2NiSi_3 and Er_2NiSi_3 exhibit a field dependent crossover from positive to negative value yielding the field induced transition from AFM to FM state. Finite negative MR value is observed for all the compounds at much higher temperatures than their respective transition temperatures due to the presence of short range magnetic interaction over a wide temperature scale. The anomalous resistivity and magnetoresistance properties reported in this work are expected to trigger an interest to map the microscopic magnetic interactions in these systems by studying detailed magnetotransport properties, preferably on single crystals.

Acknowledgement

This work has been carried out and supported through CMPID-DAE project at SINP. Work at the Ames Laboratory was supported (in part) by the Department of Energy- Basic Energy Sciences, Materials Sciences and Engineering Division, under Contract No. DE-AC02-07CH11358.

References

[1] R. A. Gordon, C. J. Warren, M. G. Alexander, F. J. DiSalvo, and R. Pöttgen, J. Alloys Comp. 248 (1997) 24.
[2] S. R. Saha, H. Sugawara, T. D. Matsuda, Y. Aoki, and H. Sato, and E.V. Sampathkumaran, Phys. Rev. B 62 (2000) 425.
[3] C. Tien, C. H. Feng, C. S. Wur, and J. J. Lu, Phys. Rev. B 61 (2000) 12151.
[4] S. Majumdar, H. Bitterlich, G. Behr, W. Löser, P. L. Paulose, and E.V. Sampathkumaran, Phys. Rev. B 64 (2001) 012418.
[5] D. Li, X. Zhao, and S. Nimori, J. Phys.: Condens. Matter 21 (2008) 026006.
[6] M. Szlawska, D. Kaczorowski, and M. Reehuis, Phys. Rev. B 81 (2010) 094423.

[7] F. Tang, M. Frontzek, J. Dshemuchadse, T. Leisegang, M. Zschornak, R. Mietrach, Jens-Uwe Hoffmann, W. Löser, S. Gemming, D. C. Meyer, and M. Loewenhaupt, Phys. Rev. B 84 (2011) 104105.
[8] Z. J. Mo, J. Shen, L. Q. Yan, X. Q. Gao, C. C. Tang, J. F. Wu, J. R. Sun, B. G. Shen, J. Alloys Comp. 618 (2015) 512.
[9] S. Pakhira, C. Mazumdar, R. Ranganathan, S. Giri, and M. Avdeev, Phys. Rev. B 94 (2016) 104414.
[10] S. Pakhira, C. Mazumdar, R. Ranganathan, and M. Avdeev, Sci. Rep. 7 (2017) 7367.
[11] S. Pakhira, C. Mazumdar, A. Basu, R. Ranganathan, R.N. Bhowmik, and B. Satpati, Sci. Rep. 8 (2018) 14870.
[12] T. Kurumaji, T. Nakajima, M. Hirschberger, A. Kikkawa, Y. Yamasaki, H. Sagayama, H. Nakao, Y. Taguchi, Taka-hisa Arima, Y. Tokura, Science 365 (2019) 914.
[13] C. Tien, L. Luo, and J. S. Hwang, Phys. Rev. B 56 (1997) 11710.
[14] A. Szytuła, M. Hofmann, B. Penc,M. Ślaski, S. Majumdar, E. V. Sampathkumaran, A. Zygmunt, J. Magn. Magn. Mater. 202 (1999) 365.
[15] D. X. Li, S. Nimori, Y. Shiokawa, Y. Haga, E. Yamamoto, and Y. Onuki, Solid State Commun. 120 (2001) 227.
[16] M. Szlawska, D. Kaczorowski, A. Ślebarski, L. Gulay, and J. Stepień-Damm, Phys. Rev. B 79 (2009) 134435.
[17] M. Szlawska, and D. Kaczorowski, Phys. Rev. B 84 (2011) 094430.
[18] R. Mallik, E. V. Sampathkumaran, M. Strecker, and G. Wortmann, Europhys. Lett. 41 (1998) 315.
[19] S. R. Saha, H. Sugawara, T. D. Matsuda, H. Sato, R. Mallik, and E. V. Sampathkumaran, Phys. Rev. B 60 (1999) 12162.
[20] S. Majumdar, M. M. Kumar, R. Mallik, and E. V. Sampathkumaran, Solid State Commun. 110 (1999) 509.
[21] S. Majumdar, R. Mallik, E. V. Sampathkumaran, K. Rupprecht and G. Wortmann, Phys. Rev. B 60 (1999) 6770.
[22] S. Pakhira, C. Mazumdar, R. Ranganathan, S. Giri, J. Alloys Comp. 742 (2018) 391.
[23] S. Pakhira, A. K. Kundu, C. Mazumdar, and R. Ranganathan, J. Phys.: Condens. Matter 30 (2018) 215601.
[24] S. Pakhira, C. Mazumdar, R. Ranganathan, S. Giri, Phys. Chem. Chem. Phys. 20 (2018) 7082.
[25] S. Pakhira, C. Mazumdar, M. Avdeev, R. N. Bhowmik, and R. Ranganathan, J. Alloys Comp. 785 (2019) 72.
[26] S. Pakhira, C. Mazumdar, D. Choudhury, R. Ranganathan, S. Giri, Phys. Chem. Chem. Phys. 20 (2018) 13580.
[27] S. Pakhira, C. Mazumdar, and R. Ranganathan, J. Phys.: Condens. Matter 29 (2017) 505801.
[28] Rodríguez-Carvajal, J. Physica B 192 (1993) 55.
[29] H. J. van Daal, and K. H. J. Buschow, phys. stat. sol. (a) 3 (1970) 853.
[30] E. V. Sampathkumaran, H. Bitterlich, K. K. Iyer, W. Löser, and G. Behr, Phys. Rev. B 66 (2002) 052409.
[31] R. J. Goetsch, V. K. Anand, A. Pandey, and D. C. Johnston, Phys. Rev. B 85 (2012) 054517.
[32] C. Mazumdar, A. K. Nigam, R. Nagarajan, L. C. Gupta, C. Godart, B. D. Padalia, G. Chandra, and R. Vijayaraghavan, Phys. Rev. B 54 (1996) 6069.
[33] C. Mazumdar, A. K. Nigam, R. Nagarajan, L. C. Gupta, G. Chandra, B. D. Padalia, C. Godart, and R. Vijayaraghavan, J. Appl. Phys. 81 (1997) 5781.
[34] H. Yamada, and S. Takada, J. Phys. Soc. Jpn. 34 (1973) 51.
[35] A. Pandey, C. Mazumdar, R. Rnganathan, and S. Dattagupta, J. Magn. Magn. Mater. 321 (2009) 2311.
[36] C. Mazumdar, A. K. Nigam, R. Nagarajan, C. Godart, L. C. Gupta, B. D. Padalia, G. Chandra, and R. Vijayaraghavan, Appl. Phys. Lett. 68 (1996) 3647.
[37] S. Nimori, and D. Li, J. Phys. Soc. Jpn. 75 (2006) 195.
[38] N. F. Mott and H. Jones, *The Theory of the Properties of Metals and Alloys* (Clarendon, Oxford, 1936).

[39] H. Wiesmann, M. Gurvitch, H. Lutz, A. K. Ghosh, B. Schwarz, M. Strongin, P. B. Allen, and J. W. Halley, Phys. Rev. Lett. 38 (1977) 782.
[40] B. Chakraborty and P. B. Allen, Phys. Rev. Lett. 38 (1979) 372.